Scripta Materialia 178 (2020) 223–226

Contents lists available at ScienceDirect

Scripta Materialia

journal homepage: www.elsevier.com/locate/scriptamat

Control of effective cooling rate upon magnetron sputter deposition of glassy $Ge_{15}Te_{85}$

Julian Pries[a], Shuai Wei[a], Felix Hoff[a], Pierre Lucas[b,*], Matthias Wuttig[a,c]

[a] Institute of Physics IA, RWTH Aachen University, 52074 Aachen, Germany
[b] Department of Materials Science and Engineering, University of Arizona, Tucson, AZ 85712, United States
[c] Peter Grünberg Institute (PGI 10), Forschungszentrum Jülich, 52428 Jülich, Germany

ARTICLE INFO

Article history:
Received 31 October 2019
Accepted 11 November 2019
Available online 22 November 2019

Keywords:
Metastable phases
Chalcogenide glasses
Glass transition
Fictive temperature
Quenching
Undercooling

ABSTRACT

Reducing the enthalpy of as-deposited amorphous films is desirable as it improves their kinetic stability and enhances the reliability of resulting devices. Here we demonstrate that $Ge_{15}Te_{85}$ glass films of lower enthalpy are produced by increasing the voltage during magnetron sputter deposition. An increase of ~100 V leads to a drop in effective cooling rate of almost three orders of magnitude, thereby yielding markedly lower enthalpy glasses. The sputtering voltage therefore constitutes a novel parameter for tuning the fictive temperature of glass films, which could help to obtain ultra-stable glasses in combination with substrate temperature control.

The fabrication of amorphous films is essential for multiple technologies ranging from integrated optics to phase change material (PCM) memory devices. Glassy (amorphous) materials are intrinsically out of thermodynamic equilibrium and their physical properties tend to evolve over time as they relax towards a lower enthalpy state [1–3]. These unwanted changes can be mitigated by producing glasses with low initial enthalpy at slow cooling rates upon vitrification, or post processing by annealing. It was also recently shown that ultra-stable glasses (USGs) can be obtained by physical vapor deposition (PVD) on substrates heated near the glass transition temperature T_g [4,5]. This phenomenon was associated with the enhanced mobility of the constituent particles on the film surface, which provided sufficient flexibility to access the lowest minima in the energy landscape. Here we investigate the effect of increasing the kinetic energy of constituent particles during magnetron sputtering of glassy $Ge_{15}Te_{85}$ films. The effective cooling rate of sputtered films is estimated by calorimetry. It is found that the final enthalpy and fictive temperature of glass films can be controlled by tuning the sputtering voltage.

While most glasses are prepared by fast cooling from the melt [6], glass films for device applications are frequently produced by PVD. In the case of PCMs, significant differences in physical properties between as-deposited and melt-quenched samples have been reported, including the atomic arrangement, the amorphous phase stability and the crystal growth velocity [7–9]. Large differences in cooling rates and vitrification processes lead to density and enthalpy changes that could account for these property modifications [10]. Yet, while the cooling rate during melt-quenching may be known, the effective cooling rate of sputter-deposited films remains unknown, rendering a comparison infeasible. It is therefore of interest to derive an effective cooling rate for as-deposited glasses. Fortunately, the cooling rate of a glass can be derived from its fictive temperature T_f, measured calorimetrically [11]. Prominent PCMs such as $Ge_2Sb_2Te_5$ or (Ag,In)-doped Sb_2Te (AIST) [12] are bad glass formers. Hence, the measurement of the glass transition temperature T_g is very challenging. On the contrary, $Ge_{15}Te_{85}$ is a good model system for a comparative study of different glassy states as it is a good glass former that exhibits a complete calorimetric glass transition [13]. This enables an unambiguous determination of T_f. It can be vitrified by cooling from the undercooled liquid (UCL) to produce glasses of known cooling rates and enthalpy for comparison with as-deposited samples (ASD). It is moreover relevant to PCMs, as it consists of the same elements as the PCM GeTe. Amorphous films of $Ge_{15}Te_{85}$ were therefore produced by magnetron sputter deposition using a sputtering power of 6–120 W corresponding to a sputtering voltage ranging from 260 to 370 V, respectively. Melt-quenched (MQ) glasses were produced for comparison with ASD glasses by heating $Ge_{15}Te_{85}$ up to well above its glass transition temperature T_g into the UCL phase and subsequently cooling at a constant rate ϑ_c of 3, 6, 10, 20 and 40 K/min in a differential scanning calorimeter (DSC).

* Corresponding author.
E-mail address: pierre@email.arizona.edu (P. Lucas).

https://doi.org/10.1016/j.scriptamat.2019.11.024

Since materials fall out of the metastable equilibrium of the UCL at different temperatures depending on ϑ_c, the enthalpy states of the resulting glasses differ [14]. If the heat capacity of the UCL is approximated as a constant $C_p^{UCL}(T) \approx const.$, where T is temperature, the enthalpy of the UCL $H^{UCL}(T)$ is a linear function in temperature. When the heat capacity of a glass $C_p^{g}(T)$ is independent of cooling rate during vitrification and approximately a constant as a function of T as well, the difference in enthalpy between two glasses i and j is given by

$$\Delta H_{g,i}^{g,j} = \Delta C_p \cdot \left(T_{f,i} - T_{f,j}\right), \tag{1}$$

where ΔC_p is the heat capacity difference between C_p^{UCL} and C_p^{g}. With these approximations $\Delta H_{g,i}^{g,j}$ is independent of temperature as long as structural relaxation is negligible. Utilizing the standard fictive temperature T_f^s of a glass formed at the standard cooling rate ϑ_c^s of 20 K/min as a reference, the enthalpy difference between a glass and the standard glass becomes [14]

$$\Delta H_g^s(T_f) = \Delta C_p \cdot \left(T_f - T_f^s\right), \tag{2}$$

which is a linear function of T_f while all other parameters are material constants. Moreover, the fictive temperature near T_f^s depends on ϑ_c according to [11,14]

$$T_f(\vartheta_c) = T_f^s \cdot \left(1 - \frac{1}{m} \cdot \log_{10}\left(\frac{\vartheta_c}{\vartheta_c^s}\right)\right)^{-1}, \tag{3}$$

where m is the fragility of the material which can be quantified by the slope in viscosity η at the standard glass transition temperature $T_g^s = T_f^s$ at 20 K/min in the so-called Angell-plot [6,15]. Therefore, ΔH_g^s is a linear function of T_f only, which itself is only a function of cooling rate ϑ_c.

In order to derive the effective cooling rate of ASD sputtered films, we first show that Eq. (2) holds for all $Ge_{15}Te_{85}$ glasses by measuring their excess heat capacity $C_p^{exc}(T)$. The excess heat capacity is the heat capacity of the crystal $C_p^{x}(T)$ curve over that of the glass or the liquid $C_p^{g,l}(T)$, $C_p^{exc}(T) = C_p^{g,l}(T) - C_p^{x}(T)$, which can be obtained from (crystal) rescan-subtracted DSC curves. It therefore constitutes the configurational component of the heat capacity by assuming that the vibrational components of the glass and crystals are equal [16,17]. As shown in Fig. 1a, upon reheating at a constant heating rate of $\vartheta_h^s = 20$ K/min, the $C_p^{exc}(T)$ curves of the MQ and ASD phases show a glass transition followed by an endothermic overshoot when entering the UCL and the UCL afterwards. Since all samples feature a glass transition, MQ and ASD $Ge_{15}Te_{85}$ are glasses at low temperatures [18]. Integrating the $C_p^{exc}(T)$-curves and normalizing them to a point in the UCL reveals the different enthalpy states of the glasses, from which ΔH_g^s is obtained, as depicted in Fig. 1b. The fictive temperature is found from the crossing point of linearly extrapolated glassy and UCL enthalpies [19], as sketched in Fig. 1b for the standard glass. The resulting ΔH_g^s values for MQ and ASD glasses show the expected linear dependence on T_f with a slope of $\Delta C_p = \Delta H_g^s/\Delta T_f = 16.9$ J mol^{-1} K^{-1} (inset of Fig. 1b), demonstrating that Eq. (2) holds. As can be seen from the inset in Fig. 1b, ΔH_g^s changes from 660 J/mol for the least stable glass, produced upon sputtering at a voltage of 257 V, to −80 J/mol for the most stable glass, prepared upon melt-quenching with a rate of 3 K/min. The total difference in ΔH_g^s hence amounts to 740 J/mol (7.6 meV/atom).

Since here ASD glasses possess higher enthalpies and fictive temperatures than the MQ states, they are considered to be less stable against relaxation [4,20,21]. As a result, ASD glasses exhibit an exothermic enthalpy release prior to the glass transition which is commonly observed in hyperquenched glasses reheated at a much smaller rate than the initial cooling rate [22]. Hence, the presence of this exothermic signature of $Ge_{15}Te_{85}$ films is indicative of a high fictive temperature and a high effective cooling rate ϑ_c^e which can be attributed to the sputtering process. Interestingly, this exothermic heat release and thus ϑ_c^e depend on the sputtering voltage U_d. To find ϑ_c^e for ASD glasses from the measured T_f values (Eq. (3)), the fragility m of the material is required. The fragility can be determined calorimetrically noting that the apparent glass transition temperature T_g is equal to the fictive temperature T_f when the subsequent heating rate ϑ_h is equal to the initial cooling rate ϑ_c upon vitrification [13,23]. In this case and after rewriting Eq. (3), the fragility m can be found from [13,14]

$$\log_{10}\left(\frac{\vartheta}{\vartheta_s}\right) = m \cdot \left(1 - \frac{T_f^s}{T_f}\right), \tag{4}$$

where $\vartheta = \vartheta_c = \vartheta_h$ and thus $T_f = T_g(\vartheta)$. Note that for non-ideally strong systems like $Ge_{15}Te_{85}$, Eq. (4) is only strictly valid for a range of T_f values near T_f^s and hence cooling rates ϑ near the standard value of $\vartheta^s = 20$ K/min. This is because m represents the slope of the viscosity-temperature dependence at $T_g^s = T_f^s$. However, in systems that exhibit non-Arrhenius behavior, this slope decreases notably at temperature much higher than T_g^s. Nevertheless, Eq. (4) is valid for heating rates accessible with conventional DSC, here 3 – 40 K/min [2]. Fitting Eq. (4) to T_f data obtained by DSC yields $m = 55$ as represented by the gray dashed line in Fig. 2. Note, that the DSC and FDSC data on $T_f(\vartheta)$ given in Fig. 2 were obtained from the glass transition temperature where the reheating rate ϑ_h is equal to the initial cooling rate ϑ_h. In addition to conventional DSC, Flash DSC (FDSC) allows for cooling and heating rates of up to 4000 K/s. Since the expected temperature gradient in the sample exceeds 5 °C above 750 K/s (see Supplementary Information (SI)), only T_f data up to that rate are considered. Now in Fig. 2, the combined DSC (circles) and FDSC (diamonds) T_f data show a curvature. This is indeed expected from the intermediate fragility of $Ge_{15}Te_{85}$. Consequently with increasing ϑ, Eq. (4) underestimates the increase in $T_f(\vartheta)$ and thus fails to describe the experimental data. This deviation becomes significant at heating rates exceeding ~ 50 K/s [2]. Therefore, Eq. (4) is extended to account for the non-Arrhenius behavior of non-ideal strong systems (fragility) based on the Vogel–Fulcher–Tammann (VFT) model of viscosity $\eta(T)$ as proposed in [24]. This extension of Eq. (4) can be given by (see SI)

$$\log_{10}\left(\frac{\vartheta}{\vartheta_s}\right) = \log_{10}\left(\frac{\eta_s}{\eta(T_f)}\right) \tag{5}$$

where η_s is the viscosity at the standard glass transition temperature T_g^s. Fitting Eq. (5) to all measured (F)DSC $T_f(\vartheta)$ data yields a fragility of 58 (Fig. 2, black dashed line) which agrees with the value obtained from low-ϑ Eq. (4) fitting and literature [13]. As an additional result from Eq. (5) fitting, viscosity values for $T = T_f$ are also derived (see SI). Contrary to Eq. (4), Eq. (5) does not deviate from the experimental data with increasing ϑ but instead reproduces the data and its curvature well. Therefore, Eq. (5) is now applied to the T_f values of the ASD phases obtained from Fig. 1 to calculate the effective cooling rate ϑ_c^e (Fig. 2). It is observed that ϑ_c^e shows a clear dependency on the sputtering voltage U_d: The lower U_d, the higher ϑ_c^e ranging from 1000 K/min (≈ 17 K/s) at 367 V and up to 200,000 K/min (≈ 3400 K/s) at 257 V. Hence, the logarithmic effective cooling rate appears to vary linearly with sputtering voltage as shown on Fig. 3. Following the indicated trend, ϑ_c^e would equal the standard cooling rate ϑ_c^s at about 470 V. Since the fictive temperature T_f depends on ϑ_c^e, T_f depends on the sputtering voltage U_d as well. This means that by increasing the sputtering voltage, the enthalpy state of the prepared glass is also lowered.

As stated earlier, when $\vartheta_c = \vartheta_h$, the measured glass transition temperature is equal to T_f. Therefore, when an ASD glass is reheated at ϑ_c^e, the measured glass transition temperature T_g should

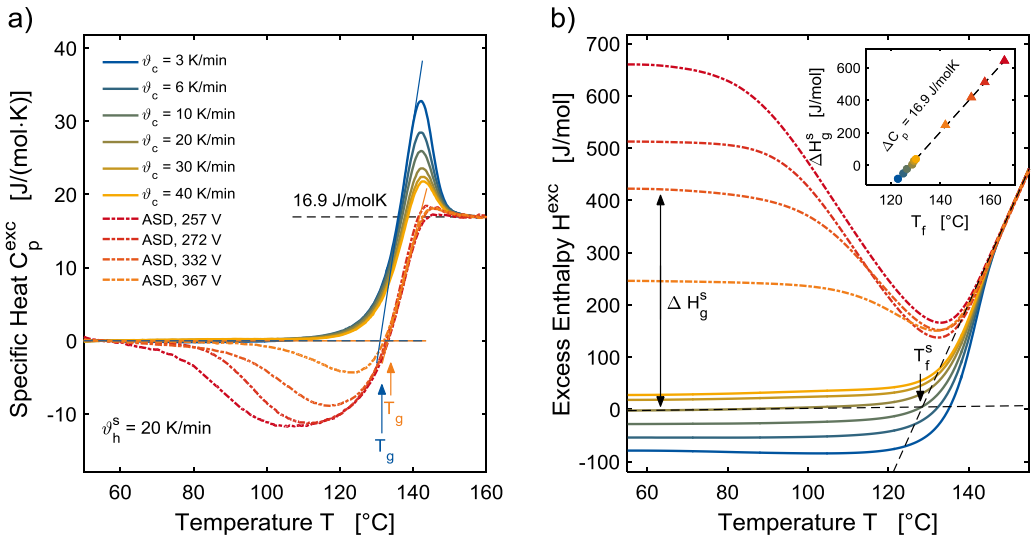

Fig. 1. Calorimetric response of melt-quenched (MQ) and as-deposited (ASD) $Ge_{15}Te_{85}$ glasses upon heating at the standard heating rate $\vartheta_h{}^s$ = 20 K/min. $C_p{}^{exc}(T)$ is the crystalline rescan-subtracted heat capacity measured in DSC. This excess heat capacity $C_p{}^{exc}(T)$ in (a) for MQ glasses shows an increased endothermic overshoot upon glass transition when the cooling rate is lowered. The endothermic overshoot is almost suppressed for ASD glasses, which instead feature a pronounced exothermic heat release prior to glass transition. This exothermic heat release is usually indicative for glasses formed with a much higher cooling rate than the subsequent heating rate. Accordingly, the exothermic heat release is absent in the slowly cooled MQ glasses. Since both, amorphous MQ and ASD $Ge_{15}Te_{85}$ show a glass transition, they have to be in the glassy state at lower temperatures. All glasses show a difference in heat capacity between the glassy and the UCL state of about 16.9 J/molK (0.175 meV/atomK). (b) From the integrated $C_p{}^{exc}(T)$ curves normalized in the UCL, the enthalpy difference between glassy states becomes apparent on the low temperature side. The enthalpy difference $\Delta H_g{}^s$ is much smaller for MQ glasses than for ASD ones, indicating that ASD glasses are less stable in this case. The fictive temperature is found at the crossing point of the extrapolated enthalpy of the glassy and UCL phase, as indicated by the arrow in (b) for the standard glass.

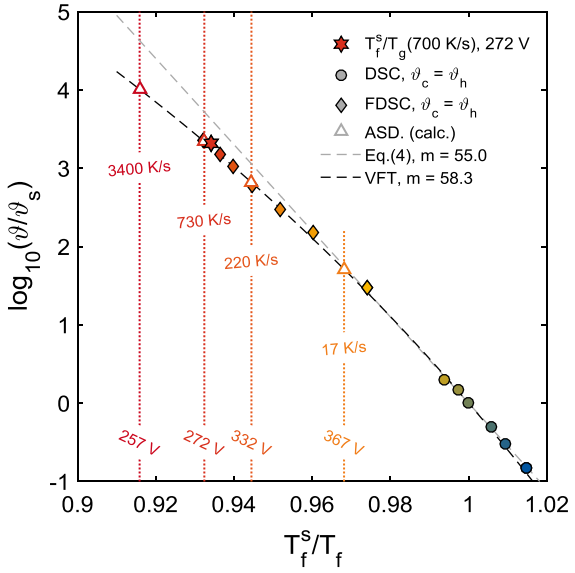

Fig. 2. Dependence of fictive temperature T_f on (effective) cooling rate ϑ_c. Axes are scaled according to Eq. (4). Additionally to the accessible cooling and heating rates in conventional DSC, measurements are extended to the rates accessible in FDSC. Here $\vartheta = \vartheta_c = \vartheta_h$, and thus the measured glass transition temperature T_g during the upscan is equal to the fictive temperature T_f of this glassy state. Heating the ASD glass prepared at 272 V at its calculated cooling rate of ~700 K/s yields $T_g \approx T_f$ (red star) and thereby verifying this argument. Eq. (4) is fitted to conventional DSC data (circles) and yields a fragility of 55 (dashed gray line). DSC and FDSC (diamonds) data is fitted by Eq. (5), which is able to describe both, the low and high rate data points, whereby a fragility of 58 is found (dashed black line). Since the fitted Eq. (5) describes the experimental data well, this formula is used to calculate the effective cooling rate $\vartheta_c{}^e$ for the ASD glassy phases from the T_f values (dotted lines) obtained from Fig. 1b (open triangles). Sputtering voltages U_d and calculated $\vartheta_c{}^e$ values for ASD $Ge_{15}Te_{85}$ are given in the figure. (For interpretation of the references to color in this figure legend, the reader is referred to the web version of this article.)

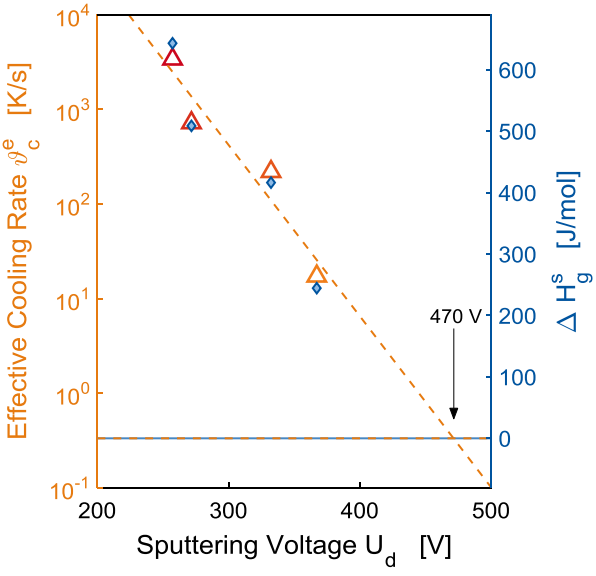

Fig. 3. Calculated effective cooling rate $\vartheta_c{}^e$ and enthalpy state $\Delta H_g{}^s$ as a function of sputtering voltage U_d. According to this extrapolation, a standard glass on an unheated substrate would be obtained at a sputtering voltage of 470 V. Furthermore, a more stable glass could be obtained at higher sputtering voltages.

be equal to T_f. To test this hypothesis, the ASD glass prepared at 272 V is heated at 700 K/s which is almost equal to its calculated $\vartheta_c{}^e$. As shown in Fig. 2, the measured T_g at that rate (red star) agrees well with the fictive temperature of that ASD glass ($C_p{}^{exc}$ curve given in the SI). This result shows that calculating the effective cooling rate $\vartheta_c{}^e$ from Eq. (5) yields reliable results for ASD glasses that were prepared not by rapid cooling but by PVD.

Our study reveals that the effective cooling rate $\vartheta_c{}^e$ of ASD glasses lays in the region of ~10^3 K/s. Another study suggests a value of ~10^4 K/s for the prominent PCM $Ge_2Sb_2Te_5$ in its glassy

ASD phase [25]. Both are far below the rate necessary for melt-quenching from above the melting temperature T_m of a PCM of ~10^9 K/s [9]. This means that $\vartheta_e{}^c$ of usual ASD glasses is about five orders of magnitude lower. Therefore, glassy PCMs obtained by melt-quenching from above T_m should thus be less stable than ASD glasses prepared by PVD. As a consequence, this should result in a higher crystal growth velocity in MQ glasses of PCMs, which explains the observation reported earlier for AIST [9].

The ability to tune the effective cooling rate $\vartheta_c{}^e$ and thus the fictive temperature T_f of the resulting glasses by controlling the sputtering voltage U_d during sputter deposition provides a novel means of adjusting the enthalpy level of the resulting as-deposited glassy phase. This finding could be exploited to help prepare ultra-stable glasses (USGs). It has been shown that USGs, i.e. glasses in a particularly low enthalpy state, can be synthesized by increasing the substrate temperature to around $T/T_g = 0.85$ during the deposition process [21]. Our study reveals an additional parameter for tuning the enthalpy state namely the sputtering voltage U_d. As reported here, a higher U_d lowers the enthalpy state of the resulting glass. A combined approach of adjusting both, the substrate temperature and the sputtering voltage may yield glassy states even lower in enthalpy. It has been suggested that USGs can form on heated substrates due to the increased mobility of constituent particles on the film surface. The added mobility enables each particle to explore a greater fraction of the energy landscape and reach a lower minimum. Extending on this interpretation it can be hypothesized that the increased kinetic energy of the particles at the surface of the film deposited at a higher voltage allows for additional exploration of the energy landscape in order to access the lowest minima and thus lower enthalpy states.

On the other hand, when rapidly quenched material is required, as for calorimetric measurements, to mimic the fast switched glassy phase of e.g., PCM memory devices, a low substrate temperature in combination with a low sputtering voltage should yield the highest enthalpy states of the resulting glass and thus should result in an *ultra-unstable* glass. This might enable bypassing the experimentally challenging task to vitrify large amounts of highly fragile and rapid crystallizing glass formers at highest cooling rates during melt-quenching. It also helps engineer the enthalpy level of the glassy state by adjusting the sputtering voltage and the substrate temperature.

Declaration of Competing Interests

The authors declare that they have no known competing financial interests or personal relationships that could have appeared to influence the work reported in this paper.

Acknowledgments

The authors acknowledge funding from the Deutsche Forschungsgemeinschaft (DFG) via the collaborative research center Nanoswitches (SFB 917). PL acknowledge funding from NSF-DMR grant#: 1832817.

Supplementary materials

Supplementary material associated with this article can be found, in the online version, at doi:10.1016/j.scriptamat.2019.11.024.

References

[1] C.T. Moynihan, in: R. Seyler (Ed.), Assignment of the Glass Transition, (Ed.), ASTM International, West Conshohocken, 1994, pp. 32–49.
[2] G.W. Scherer, Relaxation in Glass and Composites, Wiley, New York, 1986.
[3] C.A. Angell, K.L. Ngai, G.B. McKenna, P.F. McMillan, S.W. Martin, J. Appl. Phys. 88 (2000) 3113–3157.
[4] S.F. Swallen, K.L. Kearns, M.K. Mapes, Y.S. Kim, R.J. McMahon, M.D. Ediger, T. Wu, L. Yu, S. Satija, Science 315 (2007) 353–356.
[5] I. Lyubimov, M.D. Ediger, J.J. de Pablo, J. Chem. Phys. 139 (2013) 144505.
[6] C.A. Angell, Science 267 (1995) 1924–1935.
[7] J. Akola, J. Larrucea, R.O. Jones, Phys. Rev. B 83 (2011) 094113.
[8] J.Y. Raty, W. Zhang, J. Luckas, C. Chen, R. Mazzarello, C. Bichara, M. Wuttig, Nat. Commun. 6 (2015) 7467.
[9] M. Salinga, E. Carria, A. Kaldenbach, M. Bornhofft, J. Benke, J. Mayer, M. Wuttig, Nat. Commun. 4 (2013) 2371.
[10] P.G. Debenedetti, F.H. Stillinger, Nature 410 (2001) 259.
[11] C.T. Moynihan, A.J. Easteal, M.A. Bolt, J. Tucker, J. Am. Ceram. Soc. 59 (1976) 12–16.
[12] J.A. Kalb, M. Wuttig, F. Spaepen, J. Mater. Res. 22 (2007) 748–754.
[13] S. Wei, P. Lucas, C.A. Angell, J. Appl. Phys. 118 (2015) 034903.
[14] L.M. Wang, V. Velikov, C.A. Angell, J. Chem. Phys. 117 (2002) 10184–10192.
[15] R. Böhmer, K.L. Ngai, C.A. Angell, D.J. Plazek, J. Chem. Phys. 99 (1993) 4201–4209.
[16] C.A. Angell, S. Borick, J. Noncryst. Solids 307-310 (2002) 393–406.
[17] H.L. Smith, C.W. Li, A. Hoff, G.R. Garrett, D.S. Kim, F.C. Yang, M.S. Lucas, T. Swan-Wood, J.Y.Y. Lin, M.B. Stone, D.L. Abernathy, M.D. Demetriou, B. Fultz, Nat. Phys. 13 (2017) 900–905.
[18] E.D. Zanotto, J.C. Mauro, J. Noncryst. Solids 471 (2017) 490–495.
[19] C.T. Moynihan, A.J. Easteal, J. Wilder, J. Tucker, J. Phys. Chem. 78 (1974) 2673–2677.
[20] C.T. Moynihan, S.N. Crichton, S.M. Opalka, J. Noncryst. Solids 131-133 (1991) 420–434.
[21] H.B. Yu, M. Tylinski, A. Guiseppi-Elie, M.D. Ediger, R. Richert, Phys. Rev. Lett. 115 (2015) 185501.
[22] V. Velikov, S. Borick, C.A. Angell, J. Phys. Chem. B 106 (2002) 1069–1080.
[23] C.A. Angell, Chem. Rev. 102 (2002) 2627–2650.
[24] C.A. Angell, L.-M. Wang, Biophys. Chem. 105 (2003) 621–637.
[25] J. Pries, S. Wei, M. Wuttig, P. Lucas, Adv. Mater. 31 (2019) 1900784.